

# **Versatile Double Hydrophilic Block Copolymers: Dual Role as Synthetic Nanoreactor and Ionic and Electronic Conducting Layer for Ruthenium Oxide Nanoparticle Supercapacitors**

*Eunyong Seo, Taemin Lee, Kyu Tae Lee, Hyun-Kon Song and Byeong-Su Kim\**

Interdisciplinary School of Green Energy,

KIER-UNIST Advanced Center for Energy and Low Dimensional Carbon Materials Center,

Ulsan National Institute of Science and Technology (UNIST), Ulsan 689-798, Korea

E-mail: bskim19@unist.ac.kr

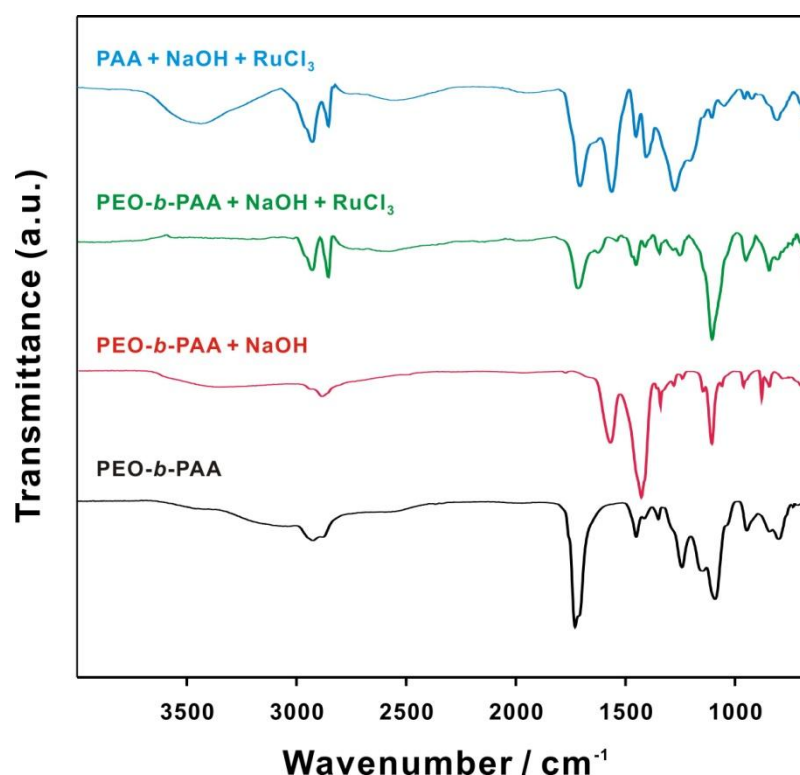


**Figure S1.** FT-IR spectra of (a) PEO-*b*-PAA, (b) PEO-*b*-PAA with NaOH, (c) PEO-*b*-PAA with NaOH and RuCl<sub>3</sub>·*x*H<sub>2</sub>O, and (d) PAA with NaOH and RuCl<sub>3</sub>·*x*H<sub>2</sub>O. Note that the PEO-*b*-PAA shows the C=O stretching vibration of the carboxylic group at 1729 cm<sup>-1</sup> and the C-O stretching vibration of PEO block and PAA block at 1241 and 1091 cm<sup>-1</sup>, respectively. Upon complexation with Ru<sup>3+</sup> through electrostatic interaction to form micellar structure, the carboxylic acid groups of PAA block are dissociated into COO<sup>-</sup> groups, which correspond to the absorption peaks at 1625 and 1410 cm<sup>-1</sup> assigned to asymmetric and symmetric stretching vibrations of COO<sup>-</sup>, while a peak of C-O observed in PEO block still remains at 1104 cm<sup>-1</sup>. This implies that the carboxylate groups of PAA block are easily involved in the reaction by combining with Ru<sup>3+</sup>. In a control experiment using only PAA polymer, the absorption peaks at 1561 and 1404 cm<sup>-1</sup> could be assigned to asymmetric and symmetric stretching vibrations of COO<sup>-</sup>, supporting carboxylate groups in PAA complex with Ru<sup>3+</sup>.

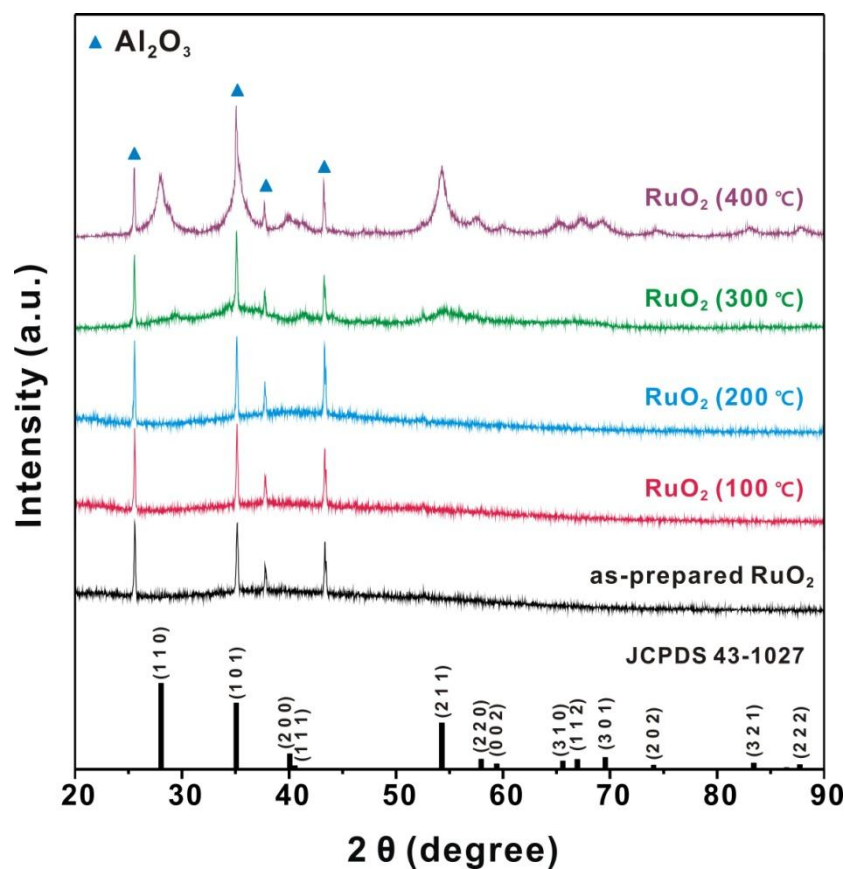


**Figure S2.** *In situ* XRD patterns of hydrous RuO<sub>2</sub>·xH<sub>2</sub>O nanoparticles with increasing temperature under ambient condition. It indicates that the crystalline RuO<sub>2</sub> structure is evolved from amorphous structure of as-prepared hydrous RuO<sub>2</sub>·xH<sub>2</sub>O near at 300 °C. Note that the peaks marked with blue triangle are assigned to the Al<sub>2</sub>O<sub>3</sub> substrate, where the sample was loaded.

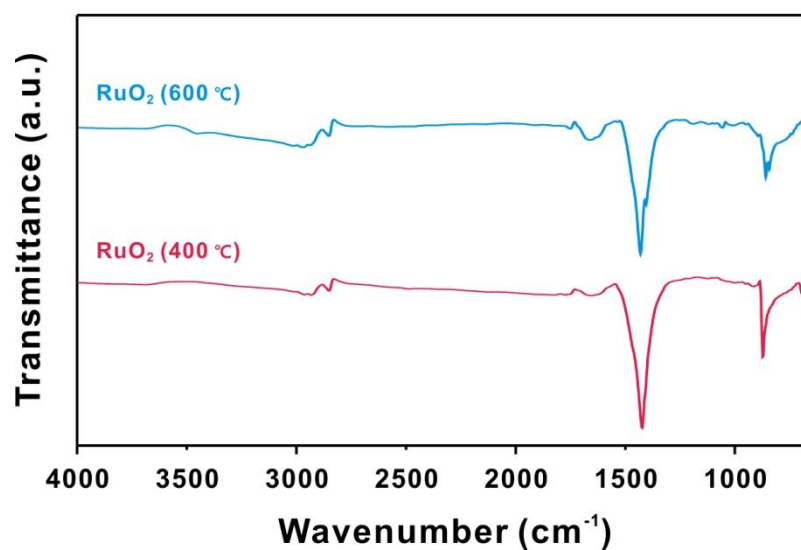


**Figure S3.** FT-IR spectra of RuO<sub>2</sub> nanoparticles annealed at 400 °C and 600 °C. Both spectra reveals the presence of residual polymeric layer, including symmetric stretching of carboxylate peaks at 1435 cm<sup>-1</sup>, which corresponds to the surface-bound strong coordinating carboxylate groups, and the other strong peak observed at 863 cm<sup>-1</sup> due to the strong rocking of methylene (-CH<sub>2</sub>-) backbone of the polymer.

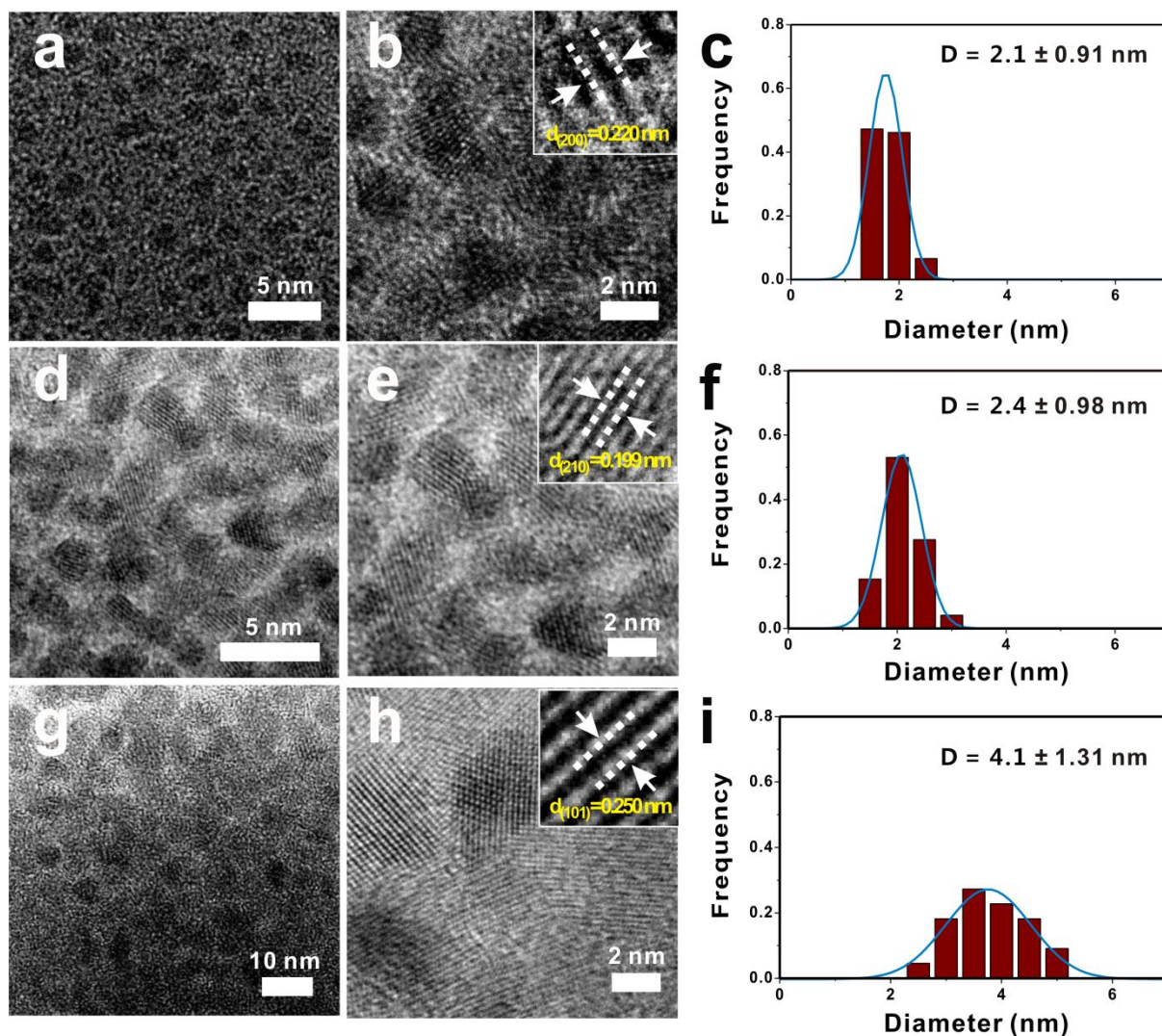


**Figure S4.** Representative TEM images of RuO<sub>2</sub> nanoparticles annealed at various temperatures. (a, b) 200 °C, (d, e) 400 °C and (g, h) 600 °C. The inset images show the crystalline plane of RuO<sub>2</sub> nanoparticles. (c, f, i) The corresponding size distribution histograms of RuO<sub>2</sub> nanoparticles averaged over 50 samples.

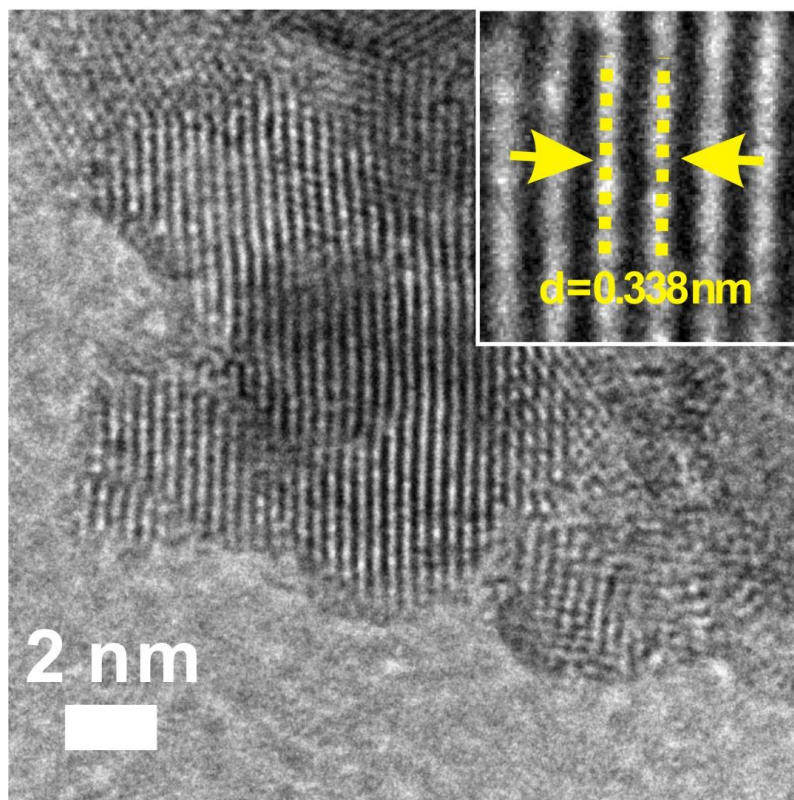


**Figure S5.** Representative HR-TEM image of RuO<sub>2</sub> nanoparticles annealed at 600 °C. Highly crystalline carbon layer is formed on the surface of RuO<sub>2</sub> nanoparticles.

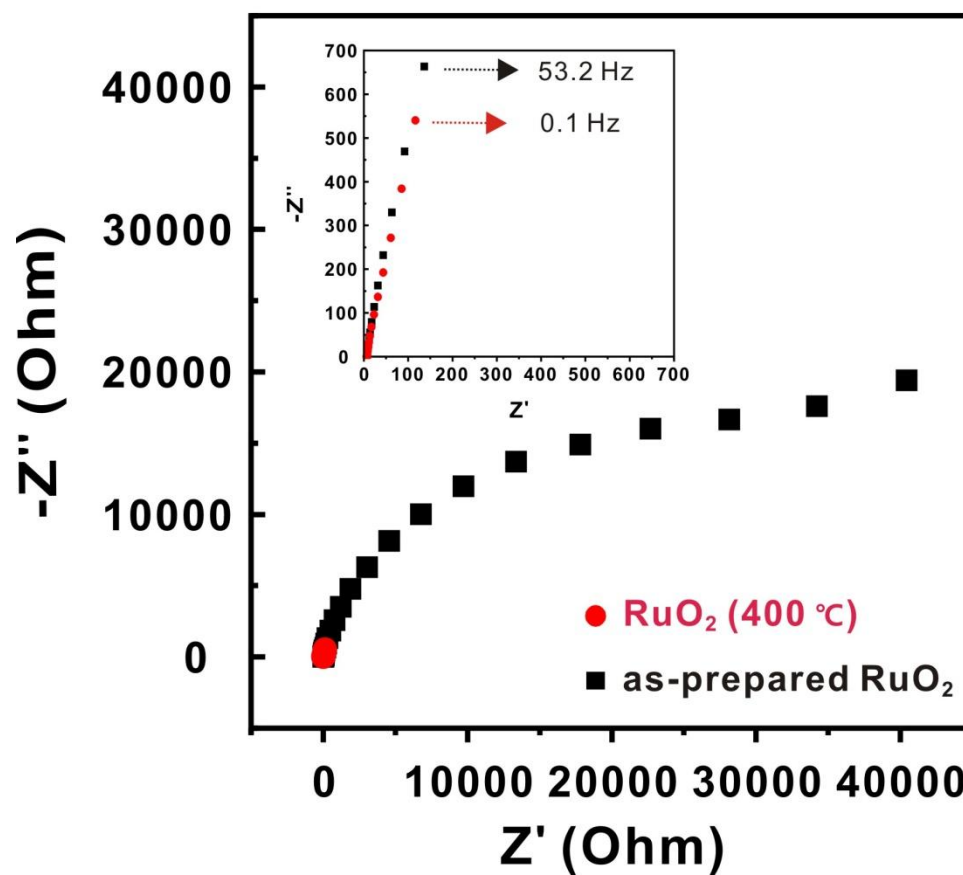


**Figure S6.** Nyquist plots for an electrode of (black square) as-prepared  $\text{RuO}_2$  and (red circle)  $\text{RuO}_2$  annealed at 400 °C, measured over a frequency range from 100 mHz to 200 kHz at 0.6 V.



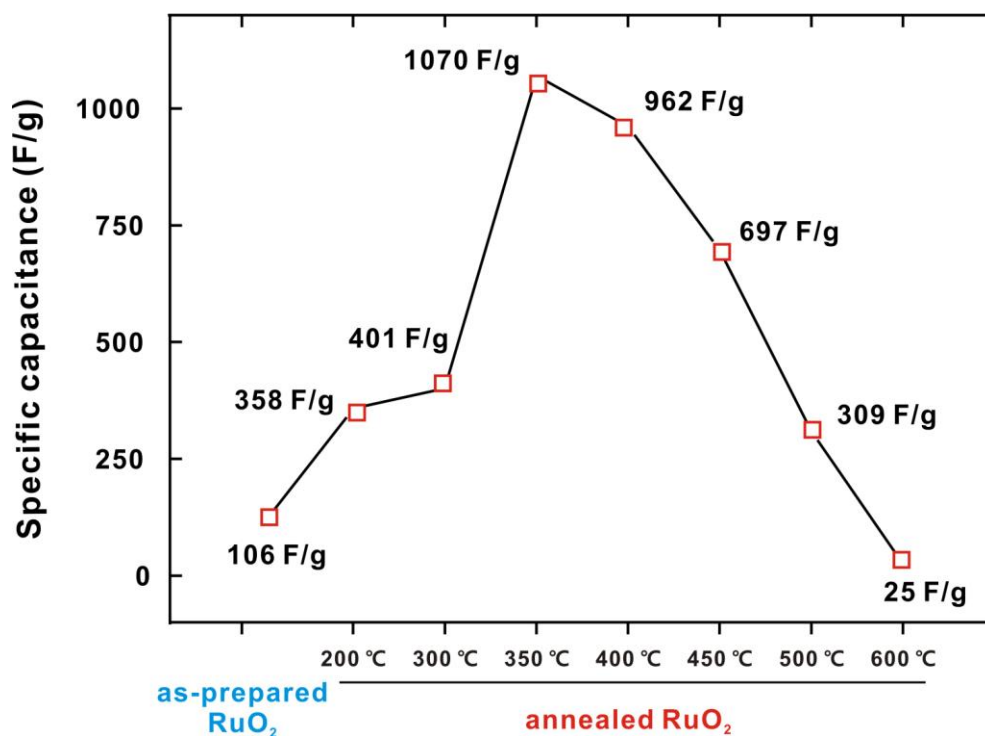


**Figure S7.** Comparison of capacitance values of all RuO<sub>2</sub> nanoparticles samples annealed at different temperature ranges. Capacitance values were obtained with a cyclic voltammetry measurement at a scan rate of 10 mV/s.



**Table 1.** Comparison of capacitance values of all RuO<sub>2</sub> nanoparticles samples annealed at different temperature ranges measured at various scan rates.

Scan rate (mV/s)	as-prepared hydrous RuO <sub>2</sub>	annealed RuO <sub>2</sub> nanoparticles						
		200 °C	300 °C	350 °C	400 °C	450 °C	500 °C	600 °C
10	106	358	401	1070	962	697	309	25
20	59	306	314	953	637	464	293	35
50	29	254	260	858	553	426	284	32
100	17	223	231	819	472	396	276	30
200	11	166	209	751	430	362	266	28